The Oxidation Mechanism of Low-Pressure Dry Oxidation of Nitrides for Memory Devices

Han-Wen Liu, Huan-Ping Su, Wen-Koi Lai, and Huang-Chung Cheng

Department of Electronics Engineering and Institute of Electronics, National Chiao Tung University, Hsinchu, Taiwan

ABSTRACT

To be utilized in the high density dynamic random access memory devices, low-pressure dry oxidation of the very thin nitrides has been performed to successfully obtain the ultrathin capacitors' dielectrics with the effective oxide thickness ($t_{ox,eff}$) of 30 ~ 60 Å. For the electrical properties, the low-pressure dry oxidized (LPDO) nitrides express thinner effective oxide thickness, lower leakage current, and higher reliability than do the atmospheric pressure dry oxidized (APDO) nitrides. After analyzing the diluted HF etching profiles, Auger electron spectrum and Fourier transform infrared spectrum data, an oxide/nitride/oxide (O/N/O) structure is realized for the LPDO samples with respect to the nitride/oxide structure for the APDO ones. This ultrathin O/N/O structure is believed to be the main cause of improving the electrical characteristics. Finally, a low-pressure enhanced oxidation model is also proposed to explain the unusual oxidation phenomenon on the top of the nitride films. The mechanisms of APDO and atmospheric pressure wet oxidation of nitride films are also compared.

Introduction

For high density dynamic random access memories (DRAMs) and metal oxide nitride oxide silicon (MONOS) memory devices, oxide/nitride (O/N) stacked dielectric formed by atmospheric pressure (AP) wet oxidizing thin Si_3N_4 in a short duration has been extensively applied due to their low defect density, low leakage current, and high reliability.[1-3] As currently practiced, the atmospheric pressure wet oxidation (APWO) imposes a limitation on the scaling of Si_3N_4 film thickness, thus on the maximum attainable capacitance. This is because thin Si_3N_4 films (~60 to 100 Å) cannot withstand an excessive oxidation.[4,5] To obtain higher cell capacitance, many techniques, such as use of Ta_2O_5 films, AP rapid thermal oxidized nitride and AP dry oxidized (APDO) nitride have been proposed.[6-8] Although Ta_2O_5 possesses a high dielectric constant (ϵ_r = 25) and is a potential substitute of the dielectric, the disadvantage of high leakage current, which degrades the device performance is inevitable. On the other hand, the AP rapid thermal oxidation and the AP dry oxidation of thin nitride possess high reliability and low defect density, but still have high leakage current. Recently, a new technique of oxidizing very thin Si_3N_4 films at low pressure in pure O_2 has been proposed to meet the scaling rule requirements.[9] This dielectric not only possesses low defect density and high reliability but also low leakage current. Nevertheless, the composition and the oxidation mechanism of the low-pressure dry oxidation (LPDO) of nitride need to be investigated for future realization. To clarify the oxidation mechanisms, both the APWO and APDO nitrides are also introduced.

Experimental

n-Type Si wafers (100) oriented, 2.5-3.5 Ω-cm,were used as the substrates. After RCA cleaning, the low-pressure chemical vapor deposited (LPCVD) nitride films were deposited at 750°C using SiH_2Cl_2/NH_3 mixture for various times. The thicknesses of all the initial nitride films were measured by an ellipsometer using a constant refractive index of 2.0. Then, some samples were atmospheric pressure dry oxidized (760 Torr) and low-pressure dry oxidized (0.5 Torr) in pure O_2 ambient at 850°C for various times. The LPDO and APDO experiments used the dry O_2 gas that was purified in exactly the same way. The only difference between the LPDO and APDO is with/without pumping system. In addition, some wafers were also wet oxidized in an atmospheric pressure pyrogenic ambient at 850°C for 5 min. After a 2500 Å thick LPCVD poly-Si was deposited and subsequently $POCl_3$ diffused at 850°C for 30 min, the metal oxide semiconductor (MOS) capacitors with various dielectrics were fabricated to compare the effects of the LPDO, APDO, and APWO.

The capacitance was measured at 1 MHz by a Keithley C-V system. The effective oxide thickness ($t_{ox,eff}$) is extracted from the capacitance by using an oxide dielectric constant of 3.9. To avoid the charge depletion effect, positive ($+V_g$) gate bias *I-V* measurement was conducted on n-type substrate. The time dependent dielectric breakdown (TDDB) characteristics were carried out by applying a constant electrical field stress over the range of +9 to +10 MV/cm at 100°C. The electrical field is equal to the applied voltage divided by the $t_{ox,eff}$. The capacitance, leakage current, and TDDB characteristics were measured on the MOS capacitors with the gate electrode area of 3.14×10^{-4} cm^2.

To realize the compositions of the dielectrics, a step-by-step diluted HF etching (HF:H_2O = 1:100) method was performed.[10] During the etching process, the samples were interrupted periodically to detect the nominal remaining thickness by the ellipsometer using the constant refractive index of 2.0. The Auger electron spectroscopy (AES) and Fourier transform infrared (FTIR) spectrum were also demonstrated to reconfirm the composition.

Results and Discussion

Electrical properties of LPDO and APDO dielectrics.— The effective oxide thicknesses of the LPDO and APDO of nitride films with various initial nitride thicknesses are listed in Table I. For the same initial nitride, the thickness difference between the LPDO and APDO specimens is little and never exceeds 6 Å. Figure 1 shows the curves of the leakage current densities *vs.* electric field for the LPDO and APDO specimens with various initial nitride thicknesses. Obviously, the LPDO samples have less current density than the APDO ones for the dielectric with the same initial nitride thickness. Moreover, the thinner the initial nitride is, the larger the difference of the current densities is for these two samples. Figure 2 demonstrates the Weibull plots of the TDDB results under a constant electric field stress of 9 MV/cm at 100°C for the LPDO and APDO specimens with the initial nitride thicknesses of 42 and 63 Å. Obviously, the LPDO specimens have higher reliability than the APDO ones and the greater improvement is observed for the thinner initial nitride. Interestingly, though the $t_{ox,eff}$ variation is little, the electrical

Table I. The effective oxide thicknesses ($t_{ox,eff}$) of the LPDO and APDO nitrides with various initial nitride thicknesses.

Initial nitride thickness (Å)	LPDO (Å)	APDO (Å)
42.0	46.1	45.9
63.1	54.2	51.1
84.3	67.8	62.3

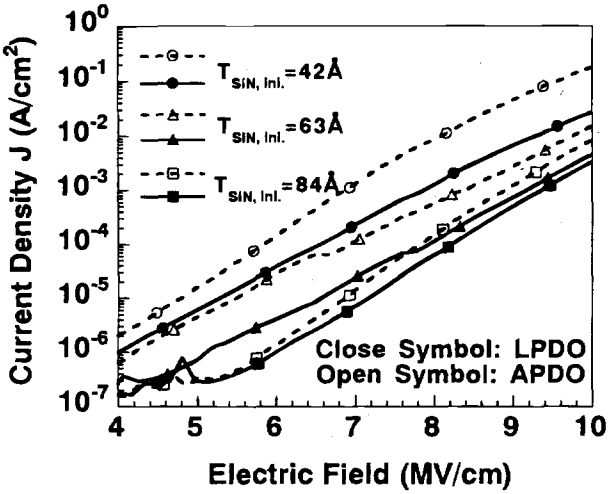

Fig. 1. The curves of the leakage current densities *vs.* electric field for the LPDO and APDO specimens with various initial nitride thickness.

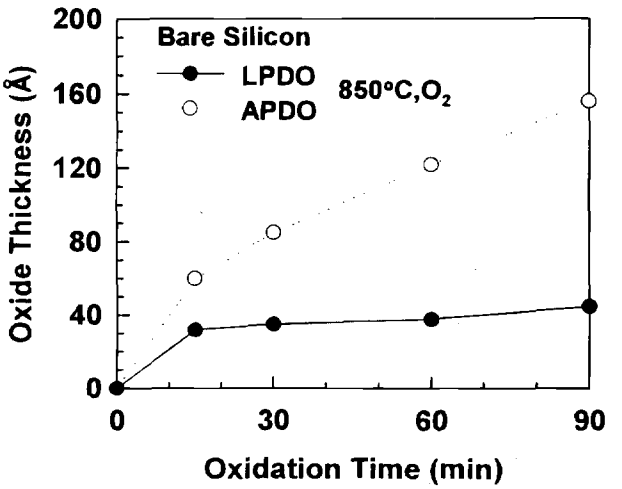

Fig. 3. The curves of oxide thickness *vs.* oxidation time for the pure oxides grown by the LPDO and APDO.

properties of the LPDO and APDO nitrides express a great difference.

The effect of oxidation time.—Except the electrical characteristics, the growth rates of LPDO and APDO nitrides are also compared. Figure 3 indicates the curves of oxide thickness *vs.* oxidation time for pure oxide grown by LPDO and APDO. The SiO_2 growth rate at atmosphere is much greater than that at 0.5 Torr. The slow growth rate of LPDO of bare silicon is due to limited number of oxidizing species. In contrast, the phenomenon of the LPDO and APDO nitrides is quite different. Figure 4 demonstrates the $t_{ox,eff}$ of the oxidized nitrides with various initial nitride thicknesses as a function of oxidation time for the LPDO and APDO. Unlike the oxidation of bare silicon, the growth rate of the LPDO specimens is higher than that of the APDO ones as the initial nitride thicknesses are 84.3 and 47.9 Å. When the initial nitride thickness is lowered down to be 34 Å, the growth rate of the LPDO specimens is relatively much slower than that of the APDO ones.

To further distinguish the mechanism of the LPDO and APDO of thin nitride, Fig. 5a and b show the $t_{ox,eff}$ increase of various nitride films as a function of oxidation time for the LPDO and APDO, respectively. Obviously, the growth rates of various nitride films under the LPDO are similar, even though the initial nitride thickness is as thin as 34 Å. On the other hand, for the APDO nitrides, the increase of the $t_{ox,eff}$ is much faster as the initial nitride is thinner. The differences between these two oxidation schemes are therefore further discussed in the next section.

Structure analysis.—For the APDO and LPDO of nitrides, all the nitride films were oxidized in the pure oxygen ambient. Therefore, it is believed that the compositions of the resultant dielectric should be the combination of oxide (SiO_2), nitride (Si_3N_4), and oxynitride (SiN_xO_y). Moslehi *et al.*[10] have proposed a step-by-step diluted HF etching method to detect the composition of

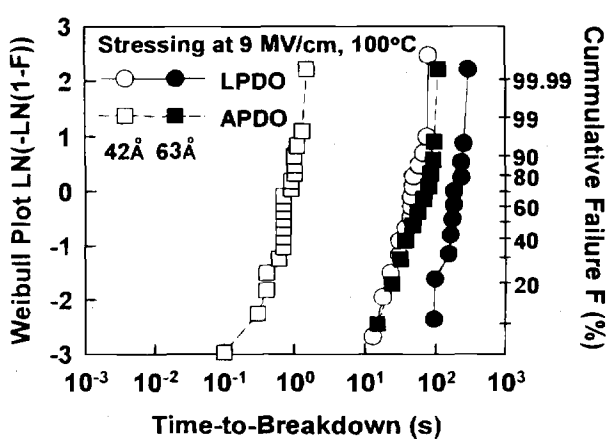

Fig. 2. The Weibull plots of the TDDB results under the constant electric field stress of 9 MV/cm at 100°C for the LPDO and APDO dielectric with the initial nitride thicknesses of 42 and 63 Å.

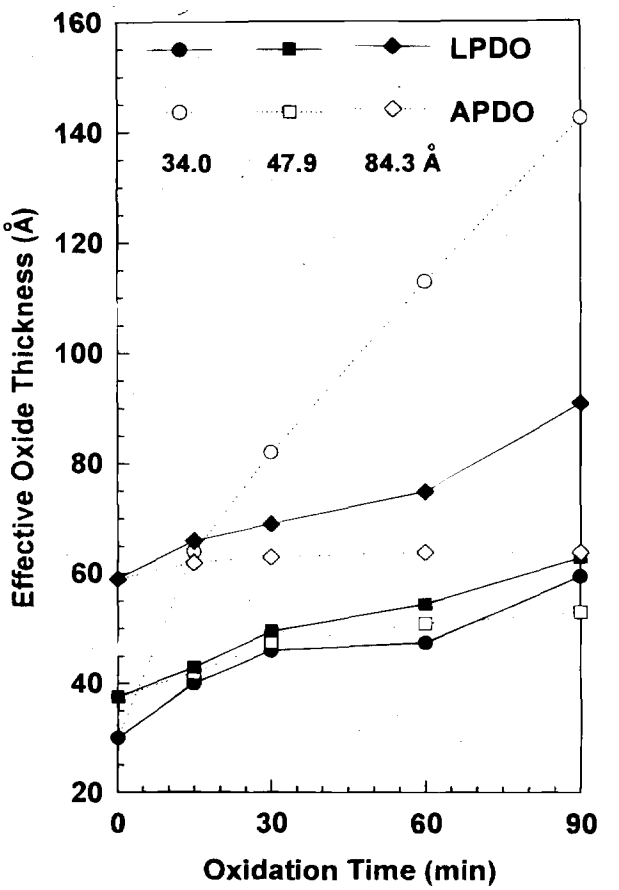

Fig. 4. The $t_{ox,eff}$ of the oxidized nitride films with various initial nitride thickness as a function of oxidation time for the LPDO and APDO.

oxidized nitride due to the different etching rates for oxide, nitride, and oxynitride. Hence, this etching method ($HF:H_2O$ = 1:100) was utilized to detect the structures of the LPDO and APDO samples. For the LPDO samples, the experiments were demonstrated at 0.5 Torr. All the samples in the tests were performed in O_2 at 850°C for 30 min. Figure 6a and b shows the nominal remaining thickness as a function of the etching time for the LPDO and APDO nitride with various initial nitride thickness, respectively. Three segments of etching rates are observed for the LPDO samples, but only two for the APDO ones. On the top of the dielectric, a fast etching rate composition is detected for the LPDO samples but not for the APDO ones. As compared with the etching rates of the pure nitride and the oxide in the same figure, it is conjectured that the oxide-like composition followed with the underlying nitride like one is obtained for the LPDO samples and only the nitride like composition is achieved for the APDO ones. In contrastly, an oxide-like bottom layer is observed for all the samples. It is well known that native oxide growth occurs before nitride deposition.[4] Therefore, in Fig. 6, the oxide-like bottom layer of the deposited Si_3N_4 should be the native oxide. As compared with the native oxide of the deposited nitride, the nominal thickness of the oxide-like bottom layer for all the oxidized nitride films are thicker. For the APDO samples, the thicknesses of the oxide-like bottom layers are becoming thicker as the initial nitride thickness decreases. This could be the reason that the $t_{ox,eff}$ of the APDO samples increases as the initial nitride is getting thinner, as shown in Fig. 5b. In contrast, the thicknesses of the oxide-like bottom layer structure for the LPDO samples are similar. Hence, as referred to the similar growth rates of the top oxide-like structure, the similar $t_{ox,eff}$ increase for various LPDO samples, as shown in Fig. 5a, can be interpreted. It is reported that oxygen can diffuse through thin nitride and form the bottom oxide.[11] Therefore, the nominal thickness increase of the bottom oxide-like structure should be the results of the reaction of diffused oxygen with silicon substrate. The retarded growth rate of the oxide-like bottom layers for the LPDO samples may be caused by the limited oxygen species at low pressure.

AES analysis.—To further investigate the three layered structure for the LPDO samples and two-layered structure for the APDO ones, the AES profiles of the LPDO and APDO nitrides with the initial nitride thickness of 63 Å on the silicon substrate are shown in Fig. 7a and b, respectively. The nitrogen profile drops significantly at the outer surface for the LPDO sample of Fig. 7a, while the nitrogen profile stays a high level at the outer surface for the APDO specimen of Fig. 7b. On the other hand, the peak of oxygen profile is high for the LPDO sample at the outer region, but a lower intensity of oxygen signal is detected for the APDO one. It depicts that the top oxide-like layer of the APDO nitride is relatively thin and not obvious, but the top oxide-like layer of LPDO ones is clear. Moreover, both the LPDO and APDO specimens exhibit an oxygen subpeak at the inner region. Consequently, combined with the previous results, an O/N/O structure for the LPDO sam-

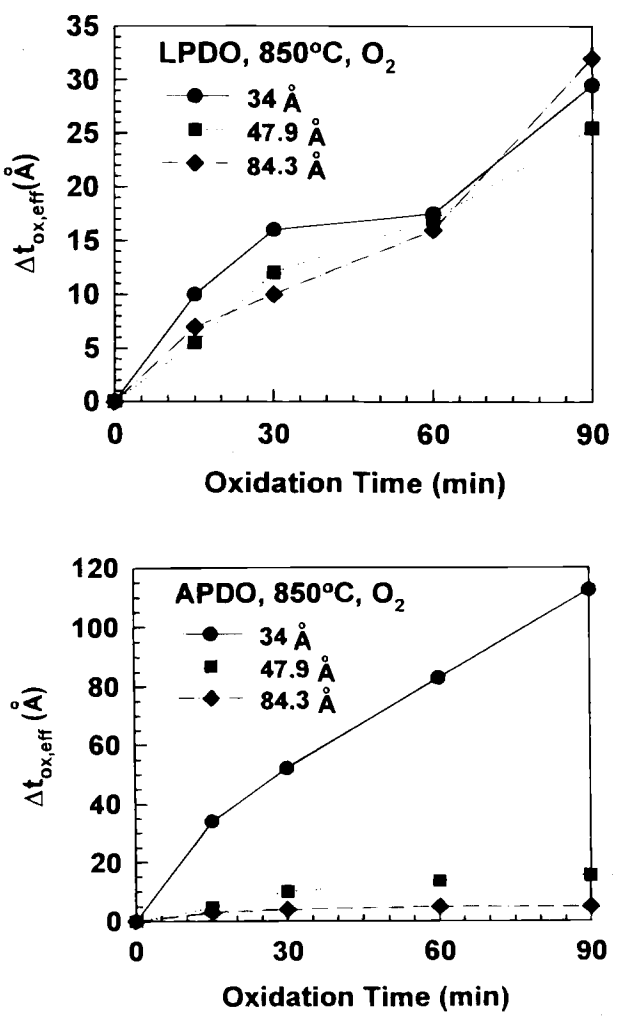

Fig. 5. The $t_{ox,eff}$ increase of various nitride films as a function of oxidation time for the (a, top) LPDO and (b, bottom) APDO samples.

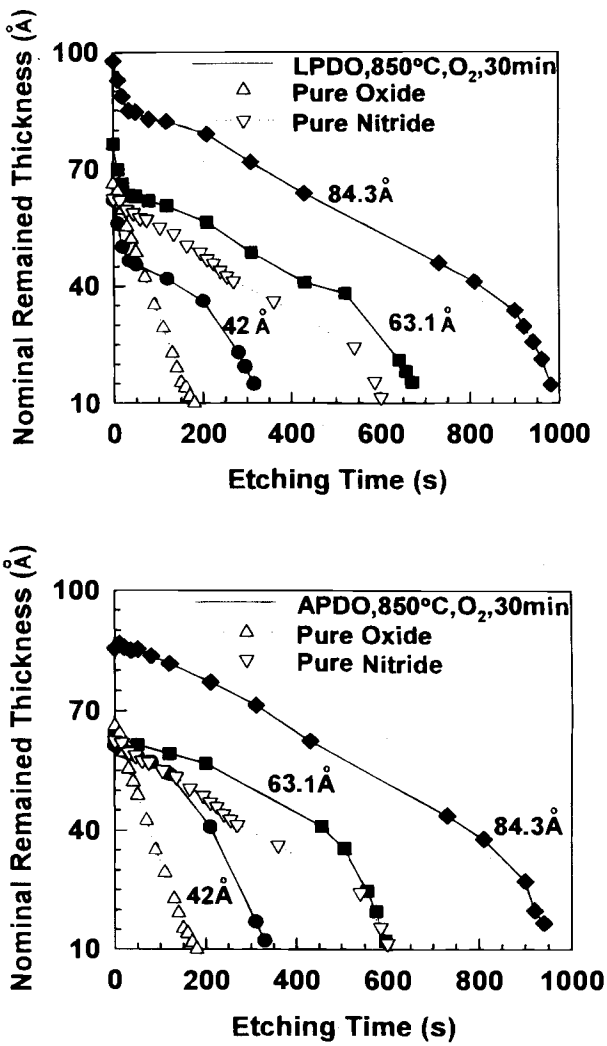

Fig. 6. The nominal remaining thickness as a function of the etching time for the (a, top) LPDO and (b, bottom) APDO nitride films with various initial nitride thicknesses.

ples and a N/O structure for the APDO ones are obtained. The O/N/O multilayer structures have been reported to achieve good barrier to the carrier injection.[2] Therefore, the formation of the O/N/O structure for the LPDO samples is the main reason to improve the electrical properties.

Analysis of the top oxide-like layer.—To confirm the composition of the top oxide, FTIR spectrum was also demonstrated. From our data, oxygen species do diffuse through thin nitride and react with the silicon substrate. To rule out this effect during analyzing the top oxide, thick nitride films were prepared for the experiments. The nitride films with the initial thicknesses of 76.4 and 210 Å were prepared for the APWO, APDO, and LPDO, accordingly. For the APWO, the nitride films were oxidized in a pyrogenic ambient for 20 min at atmospheric pressure. For the APDO and LPDO, the nitride films were oxidized in pure oxygen ambient for 60 min at 760 and 0.5 Torr, respectively. Figure 8a and b show the FTIR spectra for LPDO, APDO, and APWO samples with the initial nitride thicknesses of 76.4 and 210 Å, respectively. The data is analyzed by using the initial nitride films as the background reference. For the standard FTIR spectrum of SiO_2, the most intense mode, due to the Si-O antisymmetric stretch, is located at 1070 cm^{-1}.[12] From Fig. 8, the 1062.7 cm^{-1} peaks can be observed for both the LPDO and APWO samples even the initial nitride is thick. On the contrary, no obvious peak around 1070 cm^{-1} can be detected for the APDO specimens. It means that the composition of grown layer for the LPDO samples should have the silicon dioxide concentration like the APWO ones. The result confirms the conclusion in the previous section. To make sure of the oxide layer being grown on the top of the dielectric, the nominal remaining thickness as a function of the etching time for the LPDO specimens with the nitride thickness even of 210 Å is also indicated in Fig. 9. Clearly, a top oxide layer is still found though the initial nitride is very thick.

The oxidation of very thin nitride.—To further investigate the oxidation behavior of even thinner nitride, the 23 Å thick nitride films were oxidized at 0.5 and 760 Torr for 30 min, respectively. The effective oxide thickness of the resultant dielectric films are 51.3 and 87.4 Å for the LPDO and APDO, accordingly. These dielectric films express a great increase in thickness for both the oxidation schemes. Figure 10 shows the nominal remained thickness as a function of etching time for the LPDO and APDO specimens with the initial nitride thickness of 23 Å. The curves with only one segment of etching rate are observed for both the samples. This implies that all the nitride films have been completely transferred into the oxynitride after oxidation regardless of the oxidation techniques APDO and LPDO, leading to a significant increase of the $t_{ox,eff}$.

Discussion.—In this section, the oxidation mechanisms of the APWO, APDO, and LPDO of nitride are qualitatively discussed. Conventionally, oxidation of nitride films are demonstrated at atmosphere and well analyzed by many authors. For comparison, the degrees of the dry and wet oxidation at atmosphere should be chosen to be the same. For example, we choose that the APWO were per-

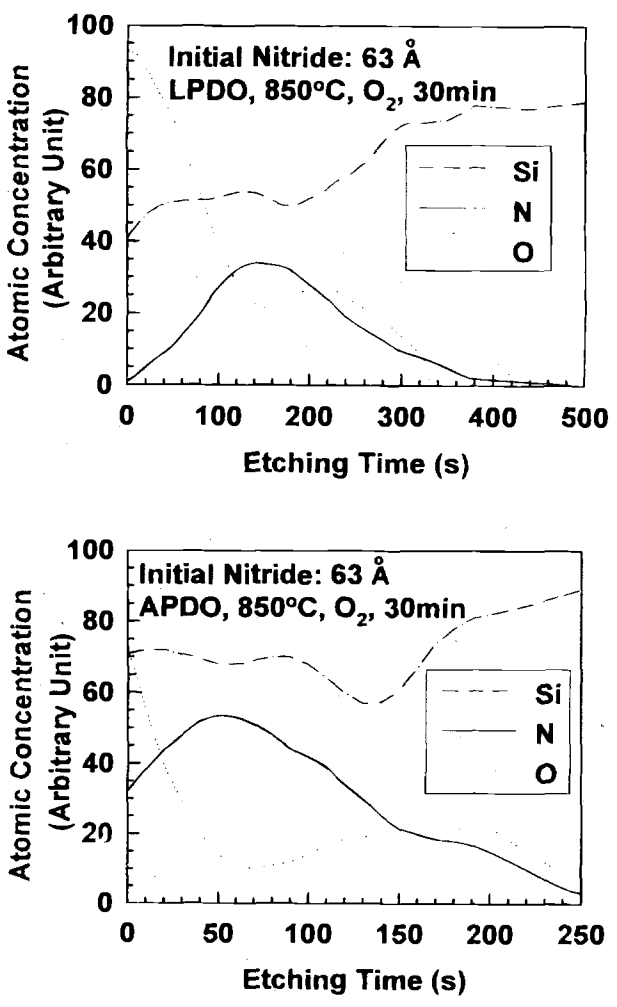

Fig. 7. The AES depth profiles of the (a) LPDO and (b) APDO nitride films with the initial nitride thickness of 63 Å on the silicon substrate.

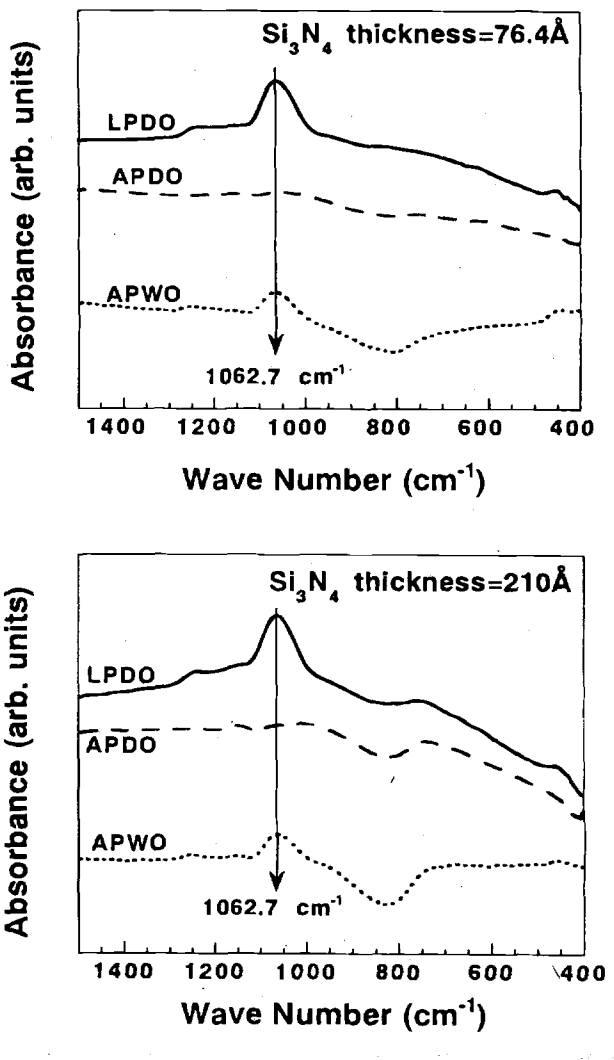

Fig. 8. The FTIR spectra for LPDO, APDO, and APWO samples with the initial nitride thicknesses of (a, top) 76.4 and (b, bottom) 210 Å.

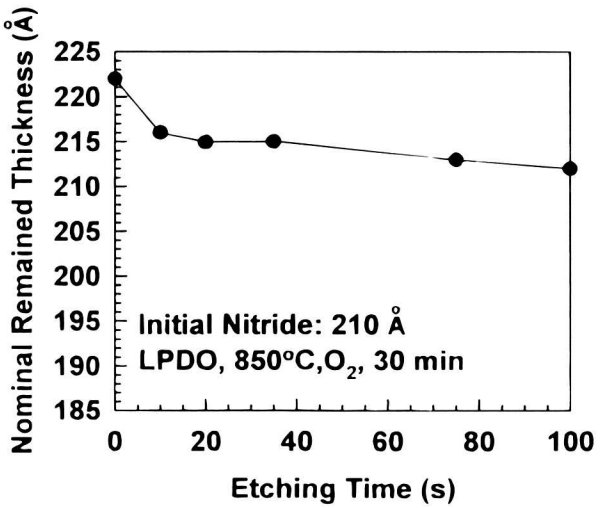

Fig. 9. The nominal remaining thickness as a function of the etching time for the LPDO of nitride with the initial nitride of 210 Å.

formed at 850°C, for 5 min in a pyrogenic ambient and the APDO were done at 850°C for 30 min in pure O_2 because about 80 Å thick SiO_2 can be grown on the Si substrate for both the conditions. For the APWO of nitride films (>>80 Å), thin SiO_2 can be grown on the top of the dielectric because hydrogen assistant oxidation occurs.[13] As the nitride thickness is getting thinner (~60 to 80 Å), except the top oxide growth, the oxidizing species can also diffuse through the dielectric easily and then react with the substrate to form the bottom oxide. Under these conditions, the AP wet oxidized nitride expresses excellent electrical properties for DRAMs' capacitors. However, as the nitride thickness is lowered down below 60 Å,[14-16] the nitride films can no longer resist the oxidation and are then transferred into the oxynitride films after the oxidation, resulting in a great increase of $t_{ox,eff}$ and not to be implemented for high density DRAMs.

In contrast, for the APDO of nitride, the very slow growth rate of the top oxide due to lack of hydrogen assistance is observed. Furthermore, like the APWO cases, the oxide-like bottom layer grows thicker as the nitride is getting thinner. Again, the nitride transfers totally into the oxynitride as the initial nitride is below 40 Å. The thinnest nitride thickness transferred into the oxynitride for the APDO conditions is less than that for the APWO ones. It is conjectured as the result of the only bottom oxide growth for the APDO nitrides.

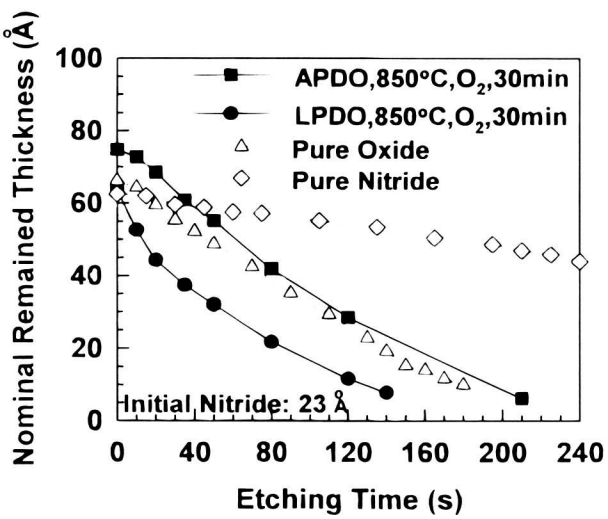

Fig. 10. The nominal remaining thickness as a function of etching time for the LPDO and APDO specimens with the initial nitride thickness of 23 Å.

Conventionally, the dry oxidation at low pressure ordinarily express a milder oxidation than that at atmosphere. That is, the APDO of nitride should express the characteristics of the nonexisting top oxide and a slow growth rate of bottom oxide-like layer. However, as for the LPDO of nitride, silicon dioxide can still grow on the top of the nitride, like the AP wet oxidation of nitride, as shown in FTIR data. It is well known that the dry oxidation of nitride can be expressed as

$$Si_3N_4(s) + 3\ O_2(g) \rightarrow 3SiO_2(s) + 2N_2(g) \qquad [1]$$

When the reaction pressure is reduced, the diffusion length of the molecules becomes longer. This is thought to be able to make the nitrogen molecules easily desorbed from the surface of the oxidized nitride. Hence, the low pressure circumstance can assist this oxidation reaction toward the right, that is favorable to the formation of the top oxide layer. On the other hand, the bottom oxide-like layer of the LPDO specimens grows with a moderate rate as the nitride films change from 80 to 40 Å. It is because of the limited supply of the oxygen for the LPDO condition. Thus, the ultrathin O/N/O stacked dielectrics which possess excellent electrical characteristics can be achieved for the LPDO of nitride. Figure 11 shows the schematic diagrams for the various initial nitride under APWO, APDO, and LPDO.

Conclusions

A novel technology for oxidizing nitride films at low-pressure in pure O_2 ambient has been proposed. It leads to the dielectric possessing the high maximum attainable capacitance, low leakage, and high reliability. To realize the oxidation mechanism of the LPDO of nitrides, the step-by-step etching tests, AES, and FTIR analysis are demonstrated. It is found that the O/N/O structure is formed for

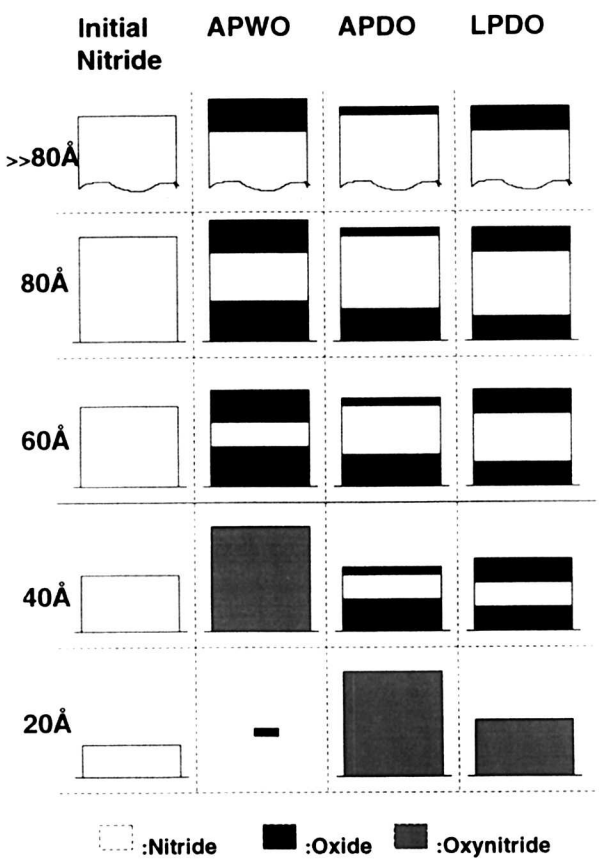

Fig. 11. The schematic diagrams for the various initial nitride under APWO, APDO, and LPDO, respectively.

the LPDO nitrides. This result is very different to the conventional APDO nitrides, in which only the N/O structure is obtained. The distinct O/N/O structure is conjectured to result in the good electrical properties for the LPDO nitrides. Finally, the oxidation mechanisms of the LPDO, APDO, and APWO of nitride films are also depicted.

Acknowledgments

This research was supported in part by the Republic of China National Science Council (ROC NSC) under the Contract No. NSC-85-2215-E009-035. Technical supports from the National Nano Device Laboratory of ROC NSC and the Semiconductor Research Center (SRC) of National Chiao Tung University are also acknowledged.

Manuscript submitted Jan. 16, 1997; revised manuscript received June 30, 1997.

National Chiao Tung University assisted in meeting the publication costs of this article.

REFERENCES

1. P. Hiergeist, A. Spitzer, and A. Rohl, *IEEE Trans. Electron Devices*, **ED-36**, 913 (1989).
2. K. Kobayashi, H. Miyatake, M. Hirayama, T. Higaki, and H. Abe, *This Journal*, **139**, 1693 (1992).
3. S. Minami and T. Kamigaki, *ibid.*, **ED-40**, 2011 (1993).
4. Z. A. Weinberg, K. J. Stein, T. N. Nuguyen, and J. Y. Sun, *Appl. Phys. Lett.*, **57**, 1248 (1991).
5. P. C. Fazan, V. K. Mathews, H. C. Chan, and A. Ditali, *IEEE Electron Device Lett.*, **EDL-13**, 86 (1992).
6. G. Q. Lo, D. L. Kwong, P. C. Fazan, V. K. Mathews, and N. Sandler, *ibid.*, **EDL-14** , 216 (1993).
7. S. Itoh, G. Q. Lo, D. L. Kwong, V. K. Mathews, and P. C. Fazan, *Appl. Phys. Lett.*, **61**, 1313 (1992).
8. W. T. Chang, D. K. Shih, and D. L. Kwong, Y. Zhou, and S. Lee, *ibid.*, **54**, 430 (1989).
9. H. P. Su, H. W. Liu, G. Hong, H. C. Cheng, *IEEE Electron Device Lett.*, **EDL-15**, 440 (1994).
10. M. M. Moslehi, C. J. Han, K. C. Sarawat, C. R. Helms, and S. Shatas, *This Journal*, **132**, 2189 (1985).
11. T. S. Chao, C. L. Lee, and T. F. Lei, *J. Appl. Phys.*, **73**, 1732 (1993).
12. T. S. Chao, W. H. Chen, and T. F. Lei, *Jpn. J. Appl. Phys.*, **34**, 2370 (1995).
13. A. E. T. Kuiper, M. F. C. Willemsen, J. M. G. Bax, and F. H. P. H. Habraken, *Appl. Surf. Sci.*, **33/34**, 757 (1988).
14. K. Ando, A. Ishitani, and K. Hamano, *Appl. Phys. Lett.*, **59**, 1081 (1991).
15. K. L. Luthra, *This Journal*, **138**, 3001 (1991).
16. P. C. Fazan, A. Ditali, C. H. Dennison, H. E. Rhodes, H. C. Chan, and Y. C. Liu, *ibid.*, **138**, 2052 (1991).

Evaluation of Polyimide Coatings Integrity by Positron Annihilation Lifetime Spectroscopy and Electrochemical Impedance Spectroscopy

M. M. Madani, H. L. Vedage, and R. D. Granata*

Zettlemoyer Center for Surface Studies, Lehigh University, Bethlehem, Pennsylvania 18015, USA

ABSTRACT

Positron annihilation lifetime spectroscopy (PALS) and electrochemical impedance spectroscopy (EIS) were used to investigate the existence of free volume cavities in polyimide coatings and the durability of these films for integrated circuits, as a function of their curing temperature. Impedance of the coatings *vs.* resistance to water uptake in the films was measured by EIS. A several orders of magnitude increase in the low frequency electrochemical impedance was observed for polyimide PI2566 (2,2′bis(3,4-dicarboxyphenyl) hexafluoroisopropylidene dianhydride + 4,4′ oxydianiline) when the coating was cured at increasing temperatures. Water exposure decreases the low frequency impedance, indicating water penetrates and changes the dielectric and conduction properties of the film. PI2566 cured above 150°C was resistant to diffusion of water after 900 h exposure. PALS showed the free volume fraction in PI2566 increased approximately 35% as a function of its curing temperature. PALS data showed three lifetimes and intensities in the polyimide specimens. There were three curing temperature regions in the free volume fraction and the average lifetime data corresponded to three imidization stages. The first region was associated with the evaporation of solvent. The second region was due to the condensation reaction (loss of water from the polyimide). A third region was related to completion of imidization. The free volume cavities increased from 46 $Å^3$ to 148 $Å^3$ with increasing curing temperature for PI2566. No large free volume cavities were found in PI2610D polyimide (pyromellitic dianhydride + oxydianiline) at curing temperatures above 150°C.

Introduction

Protection of metallic circuitry and devices from corrosion is obtained by the use of polymeric (epoxies, silicones, and polyimides) or ceramic encapsulating materials.[1] Integrated circuit (IC) chips may fail during service due to corrosion at the polymer/metal interface.[2-4] The reliability of the device depends in part on ionic contamination at the polymer metal interface.[5,6] The mechanism by which an organic coating protects a metallic material from the environment is a complex and not adequately understood process. Sorption and transfer of ions through the coating to the interface may affect corrosion behavior.[5,6] However, the concept of water absorption and transfer of ions through the coating to the interface requires that a pathway be present in the coating.[5-7] Free volume cavities in the film provide pathways, an important factor in determining the useful life of these coatings.

* Electrochemical Society Active Member.

Positron annihilation lifetime spectroscopy.—Positron annihilation lifetime spectroscopy (PALS) recently became a useful tool for investigating the existence of the free volume cavities in organic coatings.[7-9] The concept of positron backscattering from materials with a negative work-function may also be helpful in investigating the polymer/metal interface.[10]

Positrons from a radioactive source, injected into condensed matter, lose energy, reach equilibrium, and tend to bind with an electron as a positron-electron pair (a species called positronium (Ps) similar in structure to a hydrogen atom). If the positron and electron pair bind with the opposite spin, the result is a *para*-positronium (p-Ps) which annihilates in a very short period time in vacuum (0.125 ns). If the pair bind with the same spin, the result is an *ortho*-positronium (o-Ps) which annihilates in a longer time period (140 ns in vacuum). o-Ps in matter (*ex vacuo*) annihilates faster because of the pick-off process[7-9] which results from annihilation of o-Ps with an electron in sur-